

# Measuring Strain and Texture in Coatings by Using High-energy X-rays

J. Almer,<sup>1</sup> U. Lienert,<sup>1</sup> R. L. Peng,<sup>2</sup> C. Shlauer,<sup>2</sup> M. Oden<sup>2</sup>

<sup>1</sup>Advanced Photon Source, Argonne National Laboratory, Argonne, IL, U.S.A.

<sup>2</sup>Department of Mechanical Engineering, Linköping University, Sweden

## Introduction

Since the beginning of the last century, numerous attempts have been made to correlate microstructural properties, such as texture and residual stress, to macroscopic behavior in polycrystalline materials. This problem is particularly acute for coatings grown by physical-vapor deposition (PVD), which often have high levels of texture and internal stress because of the inherently nonequilibrium nature of the processes.

Here we report on high-energy x-ray diffraction measurements of PVD coatings. Transmission geometry is used with an area detector, which, as opposed to the traditional reflection geometry, allows simultaneous collection of strain and texture with direct depth resolution. Two Cr-N coatings grown at different biases (ion energies) are investigated. Previous studies on these coatings [1, 2] have shown that through substrate bias control, coatings with the same (cubic) phase and similar residual strains and chemical composition but with markedly different crystallographic texture can be grown. As such, they offer an excellent means to study the interplay between coating texture and internal strain that is needed for micromechanical modeling.

## Methods and Materials

Coatings were grown via vacuum-arc evaporation, a PVD process that utilizes a high-voltage arc to liberate particles from the anode (Cr in this case), thus creating a plasma of positively charged ions. After mechanically polishing and then sputter cleaning the plate substrates (tool steel Vanadis 6,  $25 \times 25 \text{ mm}^2$  area), nitrogen was introduced in the chamber at a pressure of 8 Pa, and Cr-N deposition was begun. Two separate depositions were carried out at substrate biases of  $V_S = -50 \text{ V}$  and  $-300 \text{ V}$ . The energy of the incident Cr and N ions is proportional to the substrate bias and thus significantly higher for the  $-300 \text{ V}$  sample. Deposition was carried out for 240 min, which produced approximately  $9.5\text{-}\mu\text{m}$ -thick coatings. Cross-sectional diffraction samples (through-thickness,  $1 \times 25.4 \text{ mm}^2$  area) were subsequently produced by electrodischarge machining.

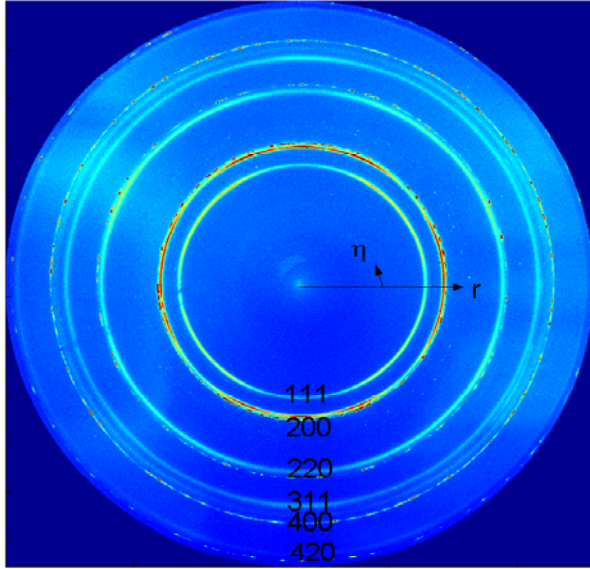
These samples were examined on the undulator line 1-ID at APS. A brilliance-preserving, double-bent Laue monochromator [3] was used to provide a high-energy ( $E = 80.72 \text{ keV}$ ) beam with a bandpass of  $\Delta E/E \sim 0.001$ . Samples were mounted with their coating/substrate

interface normal in the vertical direction ( $y$ ) and 1-mm-thick cross sections along the beam direction ( $z$ ). The transverse beam size was defined by W slits to a nominal value  $x_{\text{beam}}, y_{\text{beam}} = 100 \times 10 \mu\text{m}^2$  (vertical knife-edge scans at the sample position gave a full-width, half-maximum [FWHM] value of  $7.5 \mu\text{m}$ ). Thus the spatial resolution along the  $y$ -direction was on the order of the coating thicknesses, ensuring a good coating/substrate intensity ratio. Two-dimensional intensity was recorded with a Mar345 on-line image plate (345-mm diameter), binned to  $150\text{-}\mu\text{m}$  pixel size and located 1115 mm from the sample. Typical x-ray exposure times were 10 s, with about 100 s for detector readout.

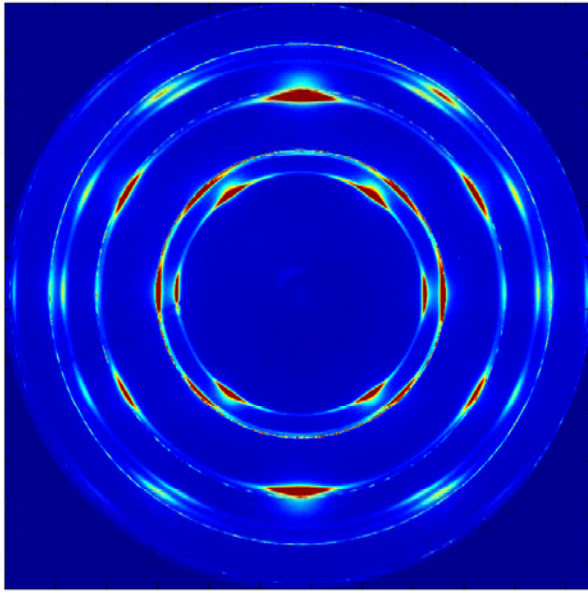
## Results and Discussion

Raw detector images from the 50-V and 300-V coatings are shown in Fig. 1. The diffraction patterns are dominated by the  $\delta$ -CrN (face centered cubic [FCC]) phase, with some slight contamination by the Fe-substrate lines (spotty peaks in figures). The 300-V sample is strongly textured ([110] along coating growth direction), while the texture for the 50-V sample is nearly random (weakly [100] along the growth direction). Lab x-ray measurements have shown that this crystallographic texture is fiber-type, such that the in-plane directions are isotropic. Under such “transverse isotropy,” the unique texture information (needed to construct an orientation distribution function [ODF]) is contained in a 2-D plane  $\mathbf{q}_{S1}\mathbf{q}_{S2}$ , where  $\mathbf{q}_{S1}$  is in-plane and  $\mathbf{q}_{S2}$  is along the growth direction. With the transmission geometry employed, the diffraction vector rotates about the detector azimuth  $\eta$  from  $\mathbf{q}_{L1}(\eta = 0, \pi) = \mathbf{q}_{S1}$  to  $\mathbf{q}_{L2}(\eta = \pi/2, 3\pi/2) = \mathbf{q}_{S2}\cos\theta_b$ , where  $\theta_b$  is the Bragg angle. The use of high energies compresses the Debye cones so that  $2 < \theta_b < 4^\circ$  with our setup, so the measurement cone  $\mathbf{q}_{L1}\mathbf{q}_{L2}$  is nearly parallel to  $\mathbf{q}_{S1}\mathbf{q}_{S2}$ . Thus the unique microstructural information can be obtained by a single exposure.

In addition to texture, orientation-dependent internal strains were determined from the radial peak positions, as follows. Before and after the coating measurements, a ceria powder sample was measured under the same conditions (beam size, sample-detector distance, x-ray energy) as those used for the coatings. By using the program Fit2d, the ceria diffraction patterns were used to calculate the beam center and correct for detector tilt and



(a)



(b)

FIG. 1. Diffraction patterns from (a) 50-V and (b) 300-V Cr-N coatings on steel substrates. Reflections for  $\delta$ -CrN (FCC) phase are shown in (a), along with definition of radial  $r$  and azimuthal  $\eta$  coordinates, where  $\eta = \{0, \pi\}$  are in-plane ( $\mathbf{q}_{S1} = \mathbf{q}_{L1}$ ). The same  $z$ -scaling was used for both images.

transform them from polar to cartesian coordinates. Binning for this transformation was  $\eta\Delta\eta = 3^\circ$  and  $\Delta r = 150 \mu\text{m}$ , which resulted in 120 1-D radial patterns. Diffraction peaks contained in these patterns were then fit to pseudo-Voigt functions, providing information about

peak position, width, shape, and integrated intensity. Knowledge of the ceria lattice parameter  $a_0$  allowed for absolute strain calibration, such that absolute strains were below  $10^{-4}$  for all reflections (hkl) and orientations  $\eta$ .

This experimental information was then used to transform and fit the diffraction patterns from the coating samples as a function of azimuth. Results for both 50-V and 300-V coatings are shown in Fig. 2, where the radial strain  $\varepsilon(\eta)$  is plotted. The lattice parameters used for calculating the unstressed radial positions  $r_0$  were  $a_0(50 \text{ V}) = 4.154 \text{ \AA}$  and  $a_0(300 \text{ V}) = 4.140 \text{ \AA}$ ; these values were used in subsequent calculations discussed below.

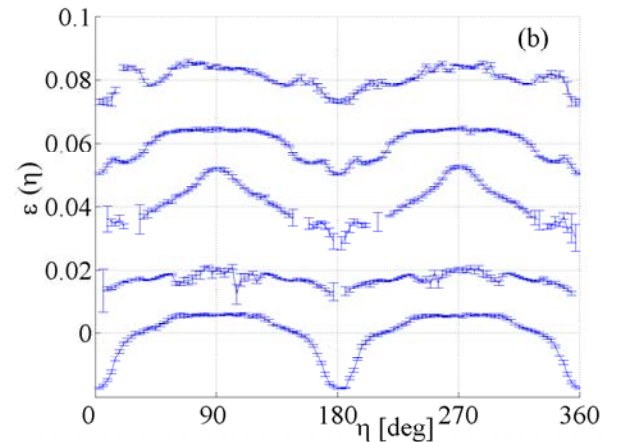
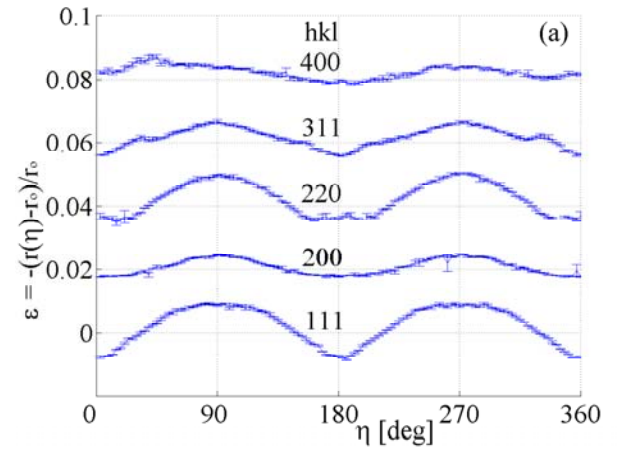


FIG. 2. Directional strain  $\varepsilon(\eta)$  for (a) 50-V and (b) 300-V  $\delta$ -CrN peaks. Error bars indicate statistical errors in each strain value, and strains are offset by 0.02 for each peak for clarity.

The figures show that considerable internal strain exists in the coatings, with maximum deviations on the order of  $\varepsilon_{max}$  of  $\sim \pm 0.01$ . The general trend is that the strain is

compressive in-plane and tensile along the growth direction. This trend is often reported in coatings grown with energetic ion bombardment (such as arc-evaporation) and has been attributed to ion implantation and resulting densification of the growing coating in a process termed “atomic shot-peening” [4]. In response to this densification, the coating attempts to hydrostatically expand but is constrained in-plane by the substrate, leading to a biaxial residual macrostress. In an isotropic medium, such a stress state would create internal strains, which vary linearly versus  $\sin^2\eta$  and are equal for each diffraction peak measured. For the Cr-N peaks, however, it is evident that the strains do not vary smoothly but instead exhibit considerable structure as a function of both orientation and hkl, especially for the more strongly textured 300-V coating.

In order to investigate this anisotropy in more detail, we attempted to fit the measured data to known micromechanical models. Reporting all the details of these calculations is beyond the scope of this article and will be published elsewhere; key features are outlined here. Two of most commonly used models, Reuss and Voigt, respectively, assume equal stress and strain in crystallites [5]. More recently, the Vook-Witt (VW) model has been developed, which assumes transverse elastic isotropy and imposes boundary conditions for stress and strain valid for thin films [6, 7]. The Voigt model predicts linear  $\epsilon\text{-}\sin^2\eta$  behavior that is clearly not valid here. Nonlinear behavior is introduced in the Reuss and VW models via crystallographic texture (ODFs) and elastic anisotropy. The VW model furthermore predicts nonlinearity even in the absence of crystallographic texture due to boundary conditions imposed [8]. Elastic anisotropy is quantified via the index  $A$ , which, for cubic systems, is:

$$A_{cubic} = 2c_{44}/(c_{11} + c_{12}),$$

where  $c_{ij}$  are the single-crystal elastic stiffnesses and  $A = 1$  for isotropy. The  $c_{ij}$  for CrN have recently been determined [9], with resultant values  $A_{\delta\text{-CrN}} = 2(88)/(542 + 27) = 0.3$ , where  $c_{ij}$  are in GPa. This value, which is comparable to measured values for other metal nitrides such as TiN, indicates high elastic anisotropy. When coupled with the ODFs (determined by using data from Fig. 1 and Beartex software), this allowed us to simulate  $\epsilon\text{-}\sin^2\eta$  patterns. Additional input to the models were  $a_0$  values (cited above) and an in-plane stress of  $-3.2$  GPa. These calculations are compared with measured data in Fig. 3.

It is clear that neither micromechanical model accurately predicts the actual strain distributions. This result is particularly surprising for the 50-V sample, which shows little texture and therefore should not be

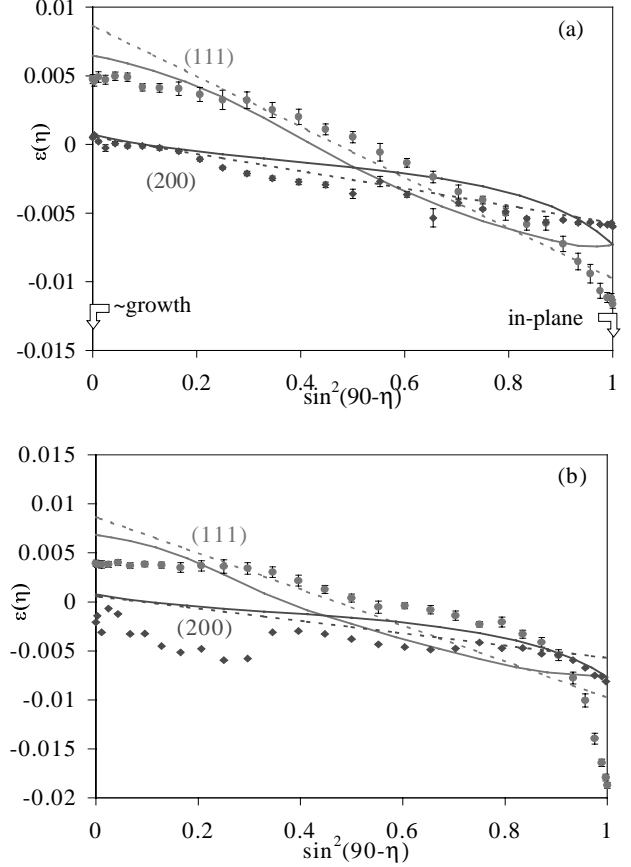


FIG. 3.  $\epsilon(\eta)$  vs. orientation for 111 and 200 reflections of (a) 50-V and (b) 300-V coatings. Data = symbols, VW = solid lines, Reuss = dotted lines.

sensitive to elastic anisotropy. Additional ion-implantation effects are being considered to interpret the measured data. In particular, we propose that the population of point defects may differ along the growth direction compared to the in-plane directions. Furthermore, the high defect densities in these coatings may be sufficient to cause alteration in the elastic behavior of arc-evaporated Cr-N relative to “defect-free” bulk CrN. Such effects are not included in any existing microstructural models.

What is apparent is that the high-energy technique presented here can be used to produce high-fidelity strain and texture data that can be used to critically test and, presumably, further develop these models.

## Acknowledgments

The authors thank G. Hankinson (Dixon Varmbehandlung AB) for advice and supplying the Cr-N coatings. Use of the APS was supported by the U.S. Department of Energy, Office of Science, Office of

Basic Energy Sciences, under Contract No. W-31-109-ENG-38.

## References

- [1] M. Odén et al., *Surf. Coat. Tech.* **114**(1), 40-52 (1999).
- [2] J. Almer et al., *J. Vac. Sci. Technol. A* **18**(1), 121-130 (2000).
- [3] S. D. Shastri et al., *APS Activity Report 1999*, pp. 258-259 (Argonne National Laboratory, Argonne, IL, 2001).
- [4] C. A. Davis, *Thin Solid Films* **226**, 30-34 (1993).
- [5] I. C. Noyan and J. B. Cohen, *Residual Stress: Measurement by Diffraction and Interpretation* (Springer-Verlag, New York, NY, 1987).
- [6] F. Witt and R. W. Vook, *J. Appl. Phys.* **39**, 2773 (1968).
- [7] M. Leoni et al., *Phil. Mag. A* **81**(3), 597-623 (2001).
- [8] M. V. Leeuwen, J.-D. Kamminga, and E. J. Mittemeijer, *J. Appl. Phys.* **86**, 1904 (1999).
- [9] M. Oden, unpublished.